Abbreviations

AISI	American Iron and Steel Institute
ALBs	Airlift bioreactors
CMC	Sodium salt of carboxymethyl cellulose
SRILAB	Split-rectangle-internal loop airlift bioreactor
NuT	Newcastle-upon-Tyne tap water

Nomenclature

a	Gas/liquid interface area (m^2 m^{-3})
$A_d/A_r^{1.618}$	Downcomer to riser area partition following the golden ratio
$A_r/A_d^{1.618}$	Riser to downcomer area partition following the golden ratio
C*	Concentration of oxygen at saturation (~8.1×10^{-3} kg m^{-3} @ 25 °C and 1 atm)
C_L	Actual dissolved oxygen concentration measured at regular intervals (kg m^{-3})
C_x	Coefficient in Equation 4
DO	Dissolved oxygen concentration (kg m^{-3})
h	Height (m)
k_L	Oxygen transfer coefficient (m s^{-1})
k_La	Overall oxygen transfer coefficient (s^{-1})
n	Exponent in Equation 4
Ø	Diameter (m)
SQ	Square cross section (m^2)
t_M	Mixing time (s)
U_G	Linear gas velocity (m s^{-1})
U_L	Linear velocity of the liquid (m s^{-1})
V_f	Final volumes (m^3)
V_i	Initial volumes (m^3)
vvm	Volume per volume per minute (m^3 min^{-1})

Greek letters

ε_g	Gas holdup (-)
ε	Gas holdup in Equation 4
μ	Dynamic viscosity (mPa.S @ 25 °C)
φ	Golden ratio [$(1+\sqrt{5})/2 = 1.618$]

Hydrodynamics of split-rectangle-internal loop airlift bioreactor with variations in riser and downcomer cross-sectional areas based on the golden ratio

Short title: Golden ratio and airlift bioreactors

Edvaldo Antonio Ribeiro Rosa[1]

Luiz Fernando Bianchini[1]

Romeu Cassiano Pucci da Silva Ramos[1]

Angela Bonjorno Arantes[1]

Roberto Francisco da Silva[2]

Jarka Glassey[3]

[1]School of Life Sciences, Pontifical Catholic University of Parana, Brazil

[2]Polytechnic School, Pontifical Catholic University of Parana, Brazil

[3]School of Engineering, Newcastle University, UK

Correspondence: Prof. Edvaldo A. R. Rosa. Xenobiotics Research Unit, Pontifical Catholic University of Parana, 1155 Imaculada Conceição St., 80215-901, Curitiba, Brazil. Email: edvaldo.rosa@pucpr.br

Keywords: Airlift bioreactor; Golden ratio, Hydrodynamic performance.

ABSTRACT

Background: The use of bioreactors that mimic industrial reality is essential if knowledge transfer is desired. This is particularly important once filamentous microbes face harsh conditions hindering the formation of biofilms in some types of bioreactors and thus diminishing their ability to perform biotransformation or production of secondary metabolites. Airlift bioreactors can circumvent such problems; however, the lack of consensus regarding riser and downcomer partition persists. The use of golden ratio is a possibility to be considered. Our proposition was to evaluate the hydrodynamic performance and mass transfer in split-rectangle-internal loop airlift bioreactors using golden ration partition. **Results:** In a general way, results revealed that a partition of $A_r/A_d^{1.618}$ presents better and more desirable characteristics than $A_d/A_r^{1.618}$ for linear liquid velocity (U_L), mixing time (t_M), gas holdup (ε_G), ~~liquid pressure (P_L),~~ and volumetric oxygen transfer coefficient (k_La). Such behavior was observed even when the SRILAB operated under different linear gas velocities (U_G) regimens (0.5 to 1.5 vvm) and Newtonian and non-Newtonian bulk fluids. **Conclusion:** Such results support the idea of using golden ratio as riser-to-downcomer partitioning parameter in airlift bioreactors.

Key words: airlift bioreactors, golden ratio, downcomer-to-riser, hydrodynamics.

INTRODUCTION

Stirred tank bioreactors are not the best options for bioprocesses involving fungi and other filamentous organisms due to high shear rates generated that compromise the morphology and/or integrity of submerged cells.[1] In this context, ~~airlift bioreactors~~ ALBs present a valuable resource for fungal growth, even as biofilm phenotype. Other advantages of ALBs include their simple design with no moving parts or agitator, easier sterilization, lower energy requirement, and greater heat-removal.[2]

Regarding hydrodynamics, variations in cross-sectional areas of riser and downcomer (A_r/A_d and A_d/A_r) are amongst the more critical parameters. Different authors report varying results in terms of the performance and cross-sectional area ratios; however, without any consensus. Most operated concentric draft tubes or external loop ALBs,[3-7] in which is more difficult to set different geometries.

To our knowledge, none has proposed using the golden ratio [$\varphi = (1+\sqrt{5})/2 = 1.618$] as parameter for A_r/A_d or A_d/A_r settings, even with sufficient evidence that it may be advantageous for fluidic systems. Different authors have shown that such proportion improves fluid mixing and should be considered for liquid systems.[8-12]

The aim of this study is to evaluate the ~~impact on~~ hydrodynamic performance when golden ratio is used as a criterion for cross-sectional areas partitioning.

MATERIALS AND METHODS

Bioreactor conception and design

One SRILAB (Figure 1A) was constructed in AISI304 stainless steel, with 0.002 m wall thickness and SQ of 0.10 m and h of 0.70 m. A flanged expansion chamber (degassing zone) of 0.25 m (SQ) × 0.15 m (h) was welded onto this column. A 0.09 × 0.025 m silicon mattress with 50 holes of 0.0005 m ø placed at the bottom of the column acted as gas sparger. The SRILAB had a working volume of 0.012 m^3.

A movable AISI304 stainless steel partition baffle of 0.65 × 0.096 mm was placed inside the column to create riser and downcomer environments. It generated a geometric operational proportion (h:SQ) of 6.5 : 1.

Two A_d/A_r were evaluated based on the golden ratio proportion (Figure 1B). The partition baffle moved forward or backward to provide two working combinations. Firstly, riser and downcomer presented SQ of 0.00618 m^2 and 0.00382 m^2 ($A_r/A_d^{1.618}$), respectively. Secondly, riser and downcomer presented SQ of 0.00382 m^2 and 0.00618 m^2 ($A_d/A_r^{1.618}$), respectively.

Determination of hydrodynamic parameters

All the tests carried out at a constant temperature of 25 ± 2 °C and 750 ± 6 mmHg.

Bulk liquids

NuT (μ = 0.89 mPa.S @ 25 °C) was used as Newtonian fluid. To mimic non-Newtonian conditions, CMC (Madhu Hydrocolloids Pvt. Ltd., India) was used at final concentrations of 0.10% (μ = 3.00 mPa.S @ 25 °C), 0.25% (μ = 7.50 mPa.S @ 25 °C) and 0.50% (μ = 15.00 mPa.S @ 25 °C). CMC solutions were prepared with NuT and their final pH were corrected to 7.0.

Airflow regimens

The SRILAB operated at five different airflow regimens: 0.50 vvm (0.006 $m^3 \cdot min^{-1}$), 0.75 vvm (0.009 $m^3 \cdot min^{-1}$), 1.00 vvm (0.012 $m^3 \cdot min^{-1}$), 1.25 vvm (0.015 $m^3 \cdot min^{-1}$), and 1.50 vvm (0.018 $m^3 \cdot min^{-1}$). Oil-free compressed air was the gas phase for all experiments.

Linear gas velocity (U_G)

This was determined by dividing the volumetric airflow ($m^3 \cdot min^{-1}$) by the cross-section area of the riser (m^2).

Linear velocity of the liquid (U_L)

The SRILAB was filled up to the working volume (0.012 m^3) with NuT. The pH values were measured by positioning the electrode tip 0.01 m bellow the liquid surface

in the riser section (Figure 1C). They were adjusted to approximately 7.00 using 1 M HCl. Air was supplied into the system at set airflow rates (see above) for 30 s. Two millilitre aliquots of 1 M HCl were carefully added in the downcomer section, 0.01 m bellow the baffle top. The mixtures were monitored by measuring the pH variations using data acquisition at one-second intervals. When pH dropped, the time interval was considered as the U_L. In contrast to other authors,[13,14] no wave-like tracer oscillations were detected in this work, but only a pattern of continuous pH drop; therefore, the alternative criteria proposed by others were used. [15]

Mixing time (t_M)

The pH drops were followed until variations became lower than 10%, when data collections were stopped. For sequential tests (not more than three repetitions for a same bulk liquid load), the pH was always adjusted to approximately 7.00 using 1 M NaOH. After achieving the desired pH, the volume was maintained constant removing excesses of liquid.

~~**Global gas retention**~~ **Gas holdup (ε_G)**

A pipe tubing manometer was built using 10 mm “speedfit pipe” and “L-elbow” connections acquired in a local hardware supplier. For measurements, a 50 mL plastic pipette was adapted after its tip had been removed (Figure 1D). The reactor was filled with NuT/CMC solutions up to the working volume and the manometer was placed in the riser section avoiding bubble entrance. The bulk liquid was aspired with a pump of an aneroid sphygmomanometer. After stabilization, initial volumes were recorded (V_i). Air was supplied into the system at set airflow rates (see above). Final volumes (V_f) were recorded after 30 s. Using the equation 1 it was possible to establish the gas holdup for each treatment.

$$\varepsilon_G = \frac{V_i}{V_i + v_f} \qquad \textbf{Eq. 1}$$

~~**Liquid pressure (P_L)**~~

~~Oscillations in bulk liquid level were converted into linear height and using the equation 2 it was possible to establish the pressure on the top after 30 s of air supply.~~

~~$P_L = \rho_L \cdot h \cdot g$~~ **~~Eq. 2~~**

~~Here, p represents pressure (Pa), ρ_m represents the liquid density (1000 kg.m^{-3}), h represents height (m), and g is acceleration due to gravity (9.81 m.s^{-2}).~~

Volumetric oxygen transfer coefficient (k_La)

The SRILAB was filled up to the working volume with either NuT or CMC solutions. pH was adjusted to approximately 7.00 using 1 M HCl. Nitrogen 5.0 was sparged into the system at a flow rate of 0.012 m^3·min^{-1} using a three-way needle valve system (Figure 1E). The drop in the dissolved oxygen concentration was measured using a DO-5509 oxygen meter (Lutron Electron. Enterp. Co. Ltd, Taiwan). After stripping the liquid of dissolved oxygen (≤ 0.3 mg·L^{-1}), the nitrogen valve was closed and air was supplied at set flow rates (see above) and the DO concentrations were measured until reach saturation steady state (normally, ~ 8.1×10^{-3} kg·m^{-3}). The increase in DO concentration was plotted against time (per second). Equation 2 was used to establish the different k_La values.

$$\ln(C^* - C_L) = -k_La \quad \textbf{Eq. 2}$$

~~In equation 3, k_L is the oxygen transfer coefficient (m·s^{-1}); a is the gas/liquid interface area (m^2·m^{-3}); k_La represents the overall oxygen transfer coefficient (s^{-1}); C* represents the concentration of oxygen at saturation (kg·m^{-3}) that is approximately 8.1×10^{-3} kg·m^{-3} at 25 °C and 1 atm; C_L is the actual dissolved oxygen concentration measured at regular intervals (kg·m^{-3}).~~ It should be noted that mass transfer experiments assume a constant k_La value in the whole reactor.

RESULTS AND DISCUSSION

General considerations

A rectangular-split architecture was used in this study due to its superior versatility and better performance characteristics for a given oxygen transfer rate.[16] In addition, industrial-sized rectangular reactors are usually easier to build and to maintain than cylindrical ones.[4,17]

Although they have some disadvantages related to the presence of possible dead zones, their geometry facilitates servicing and gives unlimited number of ratios between aerated and non-aerated compartments,[7] which are important for future improvements in performance. Finally, the rectangular-split architecture allows the accommodation of scaffolds for biofilms, which can be mounted, removed or replaced in straightforward manner.

Microbial suspensions may at times behave as pseudoplastic and present a non-Newtonian behaviour,[18] mainly when they present extracellular polysaccharides. To mimic non-Newtonian conditions, CMC was used at different concentrations. CMC solutions can model various types of non-Newtonian fluids used in many industrial processes due to their shear-thinning property[19] and to their ability to mimic sludge,[20] as well as fungal cultures.[21]

In the experiments for calculation of k_La, the gas and liquid phases were assumed as perfectly mixed and any oxygen concentration changes in the gas phase were disregarded.

Hydrodynamic parameters

Fifteen repetitions of each hydrodynamic test were performed and all data were plotted in MS-Excel® 2016 (Microsoft Co, Redmond, WA) spreadsheets. Statistical analyses were performed within SPSS 22.0 (IBM Co, Armonk, NY) using Kolmogorov-Smirnov test. Multiple comparisons were made using Tukey test at a significance level of 0.05. Table 1 shows the average and standard deviation values for all ~~hydrodynamic~~ tests assayed. For each parameter, comparisons of performance in a same fluid for different airflow (U_G) were performed. It is noticeable that most of the values of

measured/calculated variables tend to increase as a function of increments in airflow (U_G) for both $A_r/A_r^{1.618}$ and $A_d/A_r^{1.618}$. In some cases, however, such increments were not linear or even and oscillated significantly. In the case of t_M, in particular, the values drop as a function of U_G, not following the above statement. To assess the statistical significance of the differences in terms of cross-section dimensions, Student's *t* test was employed at a significance level of 0.05.

When U_G has been set as a fixed parameter, all variables analysed showed a tendency of grouping in line with their A_r/A_d and A_d/A_r architecture. Figure 2 (A to C) demonstrate this and the higher degree of homogeneity for data from $A_d/A_r^{1.618}$. However, it is possible to notice that despite the higher dispersion of data, $A_r/A_d^{1.618}$ promoted desirable overall increments in hydrodynamic parameters, as previously predicted.[13]

Variations of ε_G with U_G are shown in Figure 2A for the various CMC solutions. The figure reveals a linear development of resulting curves, contrary to observations by other authors,[15] who reported the existence of three different flow regimes for viscous solutions in split-cylinder airlift bioreactor. Such disparity between our results and those of Molina et al.[15] are likely because although both studies used viscous solutions, they applied lower U_G set points than those used by us. In addition, they used sucrose generating viscous Newtonian fluids, while CMC solutions are non-Newtonian. As stated above, CMC solutions simulate real fermentation situations.[21]

Conversely, the results presented here are similar to those obtained by others[22] with split cylinder ALB operating with U_G in a range close to those used in the current research. Overall ε_G increased approximately linearly with U_G. Such findings are interesting because linear behaviour facilitates the prediction of the fluid features in a more straightforward manner. High ε_G values may indicate that a part of the bubbles within the flow do not break at the surface and recirculate into the downcomer, increasing the mean residence time. When operating at high U_G, intensive eddy motions with high

local flow velocities may entrap some smaller bubbles within the dispersion for some time[23] ~~leading to increase in P_L (Figure 2A).~~

The geometry of riser and downcomer partition exerts a co-related influence upon t_M and U_L with trend lines for different experimental groups demonstrating opposing trends for higher concentration CMC solutions, inverted for both parameters. Reduction in t_M occurs due to increased U_L; that is why trend lines appear inverted in Figures 2B and 2C.

It is interesting to note that at $A_r/A_d^{1.618}$, solutions that are more viscous behave opposite to diluted or tap water for both parameters (no statistical analyses were carried out). On the other hand, $A_d/A_r^{1.1618}$ exerts a minor influence, regardless gas flow rate. The effect of U_G on mixing is not as significant since t_M shows a plateau (Figure 2C). Indeed, it has been already reported that higher U_G consumes more energy not necessarily improving mixing.[14]

Superficial liquid velocity and mixing time are influenced by several factors, such as U_G, viscosity/density of bulk liquid, and bioreactor geometry. In terms of the bioreactor geometry, some variables, such as the partition ratio, may interfere with the performance. For ALB operating with concentric draft tubes, risers with larger cross-section ratios promote reduction in circulation velocities; therefore gas residence times increase.[14] The results with SRILAB operating with $A_r/A_d^{1.618}$ and $A_d/A_r^{1.618}$ align with such observations (Table 1). No significant differences ($p > 0.05$) were only observed when tap water was used under an airflow rate between 0.50 vvm and 0.75 vvm.

A reduction in mixing time can be considered desirable because nutrients can be rapidly distributed, extra-cellular metabolites can be dispersed, and heat transfer can intensify.[24] However, higher U_G generates turbulence and local shear stress that can damage biofilm architecture or interfere with cellular physiology.[25] On the other hand, if U_L is low (< 0.01 m s^{-1}), gravitational sedimentation of solids may occur.[26] Since U_L values

used in these experiments were higher than the reported value, the possibility of cell deposition can be disregarded.

Volumetric oxygen transfer

To become economically viable, aerobic fermentations require a maximum rate of oxygen transfer while minimizing the power requirements. The binomial increase of k_La and reduction of air intake should always be a goal to be achieved. Results show that larger riser cross-section area ($A_r/A_d^{1.618}$ ratio) increases k_La values, regardless of the bulk liquid viscosity in a given pair of ratios ($p \leq 0.018$) (Figure 2D). A previous study[26] with SRILAB of $A_d/A_r^{1.000}$, $A_d/A_r^{0.810}$, and $A_d/A_r^{0.650}$ had already shown that k_La increases with decreasing A_d/A_r ratio. As heterogeneous flow for ε_G, caused by bubble coalescence that reduces area for mass transference and increases turbulence,[27] was not detected, it is assumed that the increased residence time of air bubbles ascending in a less turbulent flow in the $A_r/A_d^{1.618}$ ratio contributed to higher k_La values. This A_r/A_d ratio is sufficiently close to 1.650[26] to propose that the maximum performance may be near such range. In a diverse way, it was reported previously that ALBs with rectangular geometry but without gas-liquid separator tend to achieve higher k_La with $A_d/A_r^{2.000}$.[7] Possibly, the presence of the gas-liquid separator expansion on the downcomer side of our SRILAB had facilitated the gas disengagement and eliminated gas stagnation in the upper portion of the bioreactor,[26,28] what can explain such differences.

As expected, viscosity influenced the k_La for a same cross-sectional area, requiring higher flow rates of air to increase values. However, in some cases, k_La increases were not significant.

Linear trendline equations derived from plotting k_La vs ε_G indicated that $A_r/A_d^{1.618}$ ratio leads to a higher oxygen transfer rate due to the longer residence time (Figure 3). Comparatively, when the larger cross-section was the riser, the equations indicated higher coefficients for each pair in a same bulk fluid. Indeed, $A_d/A_r^{1.618}$ ratio generated even negative coefficient when NuT was used.

Exponential equations to express correlation between k_La and ε_G[29] were obtained after compiling all data in a same graph as continuous data and the equation (Eq. 3) is presented.

$$k_La = C_x \times \varepsilon^n \quad \textbf{Eq. 3}$$

~~In such equation, k_La is the volumetric oxygen transfer coefficient (s^{-1}); C_x is the coefficient; ε is the gas holdup; n is the exponent~~. Resulting equations are $k_La = 0.0570\varepsilon_G^{0.1646}$ for $A_r/A_d^{1.618}$ and $k_La = 0.0207\varepsilon_G^{-0.0170}$ for $A_d/A_r^{1.618}$. The $A_r/A_d^{1.618}$ ratio definitely presented better results.

As it can be expected, the results showed that the continuous transfer of oxygen is superior when the larger cross-section is used as riser. Indeed, attempts to improve k_La in airlift reactors shall focus on enhancement of gas holdup.[30]

Limitations

This study was limited to comparing riser and downcomer partitioning based on the golden ratio. It was not the idea to compare other architectures, once the possibilities could be enormous. Indeed, there is a consensus amongst authors that increasing SQ in riser area hydrodynamics become more favourable;[13,26] however, there is a lack of consensus about which A_d/A_r or A_r/A_d is more beneficial. Our modest contribution is restricted to evaluating differences between two partitioning systems based on the premise that the golden ratio may help to solve this impasse. Obviously, more data are required to establish the best combination.

Small ALBs usually can be assumed as ideally mixed tanks when operating with Newtonian liquid and high volumetric input gas flow, but scale up based on data from them can be difficult, mainly when three-phase systems are involved.[31] However, once fixed the conditions, hydrodynamic parameters tend to be improved in bigger ALBs. This can occur due the smaller specific friction against liquid circulation in bigger reactor scales.[32] The central idea of this study was to evaluate the plausibility of using golden

ratio in ALBs. Based on results obtained here, bench-to-plant scaling up studies can be designed to verify its industrial applicability.

CONCLUSIONS

Once the same input airflow rate was established, hydrodynamic parameters were measured for two ratio conditions, $A_r/A_d^{1.618}$ and $A_d/A_r^{1.618}$. The performance for the first condition was superior for ε_G and k_La. Values for t_M and U_L were better for the second condition.

Based on the obtained results, it is possible to conclude that SRILAB with partitioning following the golden ratio ($A_r/A_d^{1.618}$) seems to be a suitable engineering solution.

~~Hydrodynamic evaluations were carried out with tap water (Newtonian fluid) and carboxymethyl cellulose (CMC) solutions at different concentrations (non-Newtonian fluid). In general, the hydrodynamic parameters were more affected by the cross-section ratio architecture than by the rheological characteristics of bulk fluids.~~

~~For biotechnological purposes, the most important feature is the ability to supply oxygen to satisfy cellular demands in a constant manner. Thus, k_La is the most important parameter and evaluated in the research reported here. The results observed here are in agreement with results reported previously and indicate a close relationship between U_G and k_La. Such relationship corroborates for better performance of $A_r/A_d^{1.168}$ cross-section ratio.~~

ACKNOWLEDGEMENT

The authors wish to thank the Newton Fund/Royal Academy of Engineering that supplied the fellowship grant (NRCP1617/6/215).

ETHICAL APPROVAL

This article does not contain any studies with human participants or animals performed by any of the authors.

CONFLICT OF INTEREST

The authors declare no financial or commercial conflict of interest.

REFERENCES

1. Merchuk J, Why use airlift bioreactors? *Trend Biotechnol* **8:**66–71 (1990).
2. Margaritis A and Wallace JB, Novel bioreactor systems and their applications. *Nat Biotechnol* **2:**447–453 (1984).
3. Gavrilescu M and Tudose RZ, Concentric-tube airlift bioreactors. Part III: Effects of geometry on mass transfer. *Bioproc Eng* **19:**175–178 (1998).
4. Petersen EE and Margaritis A, Hydrodynamic and mass transfer characteristics of three-phase gaslift bioreactor systems. *Crit Rev Biotechnol* **21:**233–294 (2001).
5. Klein J, Vicente AA and Teixeira JA, Hydrodynamic considerations on optimal design of a three-phase airlift bioreactor with high solids loading. *J Chem Technol Biotechnol* **78:** 935–944 (2003).
6. Roy S, Dhotre MT and Joshi JB, CFD simulation of flow and axial dispersion in external loop airlift reactor. *Chem Eng Res Design* **84:**677–690 (2006).
7. Dandrev S, Pevev KI and Karamanev D, Study of the hydrodynamics and mass transfer in a rectangular airlift bioreactor. *Chem Eng Sci* **146:**180–188 (2016).
8. Mokry M, Encounters with the golden ratio in fluid dynamics. *WIT Trans Ecol Environ* **114**119–128 (2008).
9. Wang JF, Liu Y and Xu YS, The golden-mean surface pattern to enhance flow mixing in micro-channel. *Biomed Microdevices* **11:**351–357 (2009).
10. Rosson BT, Characteristic equations with solutions that contain nature's golden ratio. *WIT Trans Ecol Environ* **138:**153–163 (2010).

11. Inoue Y, Kawazoe H, Yamada M and Hirata Y, Fluid mixing and golden ratio condition. *Kagaku Kogaku Ronbun* **40:**449–461 (2014).
12. Walker JA, Golden ratio axial flow apparatus. US Patent N° 9,328,717 (2016).
13. Gavrilescu M and Tudose RZ, Effects of downcomer-to-riser cross sectional area ratio on operation behavior of external-loop airlift bioreactors. *Bioproc Biosyst Eng* **15:**77–85 (1996).
14. Yakubo-Gumery F, Ein-Mozaffari F and Dahman Y, Macromixing hydrodynamic study in draft-tube airlift reactors using electrical resistance tomography. *Bioproc Biosyst Eng* **34:** 135–144 (2011).
15. Molina E, Contreras A and Chisti Y, Gas holdup, liquid circulation and mixing behavior of viscous Newtonian media in a split-cylinder airlift bioreactor. *Chem Eng Res Design (Trans IChemE)* **77:**27–32 (1999).
16. Merchuk J and Gluz M, Bioreactors, airlift reactors. In: *Encyclopedia of bioprocess technology: fermentation, biocatalysis and bioseparation,* vol 1, ed by Flickinger MC and Drew SW. John Wiley & Sons, New Jersey, pp 320–353 (1999).
17. Couvert A, Roustan M and Chatellier P, Two-phase hydrodynamic study of a rectangular airlift loop reactor with an internal baffle. *Chem Eng Sci* **54:**5245–5252 (1999).
18. Doran PM, *Bioprocess engineering principles*. Academic Press Ltd, London, 926 p (2012).
19. Li S, Ma Y, Fu T, Zhu C and Li H, The viscosity distribution around a rising bubble in shear-thinning non-Newtonian fluids. *Braz J Chem Eng* **29:**265–274 (2012).
20. Eshtiaghi N, Yap SD, Markis F, Baudez JC and Slatter P, Clear model fluids to emulate the rheological properties of thickened digested sludge. *Water Res* **46:**3014–3022 (2012).

21. Pedersen AG, Bundgaard-Nielsen M, Nielsen J, Villadsen J and Hassager O, Rheological characterization of media containing *Penicillium chrysogenum*. *Biotechnol Bioeng* **41:**162–164 (1993).
22. Orazem ME, Fan LT and Erickson LE, Bubble flow in the downflow section of an airlift tower. *Biotechnol Bioeng* **21:**1579–1606 (1979).
23. Sieblist C and Lübbert A, Gas holdup in bioreactors. In: *Upstream Industrial Biotechnology*, vol 2. Ed by Flickinger MC. John Wiley & Sons, New Jersey, pp 1137-1146 (2013).
24. Pakula R and Freeman A, A new continuous biofilm bioreactor for immobilized oil-degrading filamentous fungi. *Biotechnol Bioeng* **49:**20–25 (1996).
25. Garcia-Ochoa F and Gomez E, Bioreactor scale-up and oxygen transfer rate in microbial processes: an overview. *Biotechnol Adv* **27:**153–176 (2009).
26. Tobajas M, Siegel MH and Apitz SE, Influence of geometry and solids concentration on the hydrodynamics and mass transfer of a rectangular airlift reactor for marine sediment and soil bioremediation. *Can J Chem Eng* **77:**660–669 (1999).
27. Rossi MJ, Nascimento FX, Giachini AJ, Oliveira VL and Furigo Jr A, Airlift bioreactor fluid-dynamic characterization for the cultivation of shear stress sensitive microorganisms. *J Adv Biotechnol* **5**:640–651 (2016).
28. Siegel M and Merchuk JC, Hydrodynamics in rectangular air-lift reactors: scale-up and the scale-up and the influence of gas-liquid separator design. *Can J Chem Eng* **69:**465–473 (1991).
29. McManamey WJ and Wase DAJ, Relationship between the volumetric mass transfer coefficient and gas holdup in airlift fermentors. *Biotechnol Bioeng* **28:**1446–1448 (1986).
30. Chisti MY and Moo-Young M, Hydrodynamics and oxygen transfer in pneumatic bioreactor devices. *Biotechnol Bioeng* **1:**487–494 (1988).

31. Heijnen JJ, Hols J, van der Lans RGJM, van Leeuwen HLJM, Mulder A and Weltevrede R. A simple hydrodynamic model for the liquid circulation velocity in a full-scale two- and three-phase internal airlift reactor operating in the gas recirculation regime. *Chem Eng Sci* **52**:2527-2540 (1997).
32. BlažejM, Kiša M and Markoš J. Scale influence on the hydrodynamics of an internal loop airlift reactor. *Chem Eng Process* **43**: 1519–1527 (2004).

Table 1. Values for different hydrodynamic and mass transfer variables.

Air flow	vvm	0.50	0.75	1.00	1.25	1.50	Bulk
	$m^3\ min^{-1}$	0.006	0.009	0.012	0.015	0.018	
ε_G (-)	$A_r/A_d^{1.618}$	0.112 ± 0.002 A*	0.139 ± 0.002 B*	0.165 ± 0.002 C*	0.189 ± 0.003 D*	0.213 ± 0.003 E*	NuT
	$A_d/A_r^{1.618}$	0.020 ± 0.001 A	0.038 ± 0.001 B	0.056 ± 0.001 C	0.074 ± 0.001 D	0.075 ± 0.001 D	
	$A_r/A_d^{1.618}$	0.020 ± 0.001 A*	0.038 ± 0.001 B*	0.074 ± 0.001 C*	0.107 ± 0.001 D*	0.152 ± 0.002 E*	0.10% CMC
	$A_d/A_r^{1.618}$	0.012 ± 0.001 A	0.019 ± 0.001 B	0.038 ± 0.001 C	0.056 ± 0.001 D	0.074 ± 0.001 E	
	$A_r/A_d^{1.618}$	0.091 ± 0.002 A*	0.094 ± 0.001 A*	0.107 ± 0.001 B*	0.123 ± 0.002 C*	0.153 ± 0.002 D*	0.25% CMC
	$A_d/A_r^{1.618}$	0.020 ± 0.001 A	0.030 ± 0.001 B	0.038 ± 0.001 C	0.056 ± 0.001 D	0.074 ± 0.001 E	
	$A_r/A_d^{1.618}$	0.090 ± 0.002 A*	0.107 ± 0.001 B*	0.152 ± 0.002 C*	0.166 ± 0.002 D*	0.194 ± 0.003 E*	0.50% CMC
	$A_d/A_r^{1.618}$	0.038 ± 0.002 A	0.056 ± 0.001 B	0.074 ± 0.001 C	0.091 ± 0.001 D	0.123 ± 0.002 E	
U_L ($m\ s^{-1}$)	$A_r/A_d^{1.618}$	0.199 ± 0.004 A^0	0.199 ± 0.003 A^0	0.133 ± 0.002 B	0.160 ± 0.002 C	0.160 ± 0.002 C	NuT
	$A_d/A_r^{1.618}$	0.199 ± 0.004 A	0.199 ± 0.003 A	0.266 ± 0.003 B*	0.266 ± 0.001 B*	0.267 ± 0.003 B*	
	$A_r/A_d^{1.618}$	0.159 ± 0.003 A	0.133 ± 0.002 B	0.114 ± 0.001 C	0.133 ± 0.002 B	0.133 ± 0.002 B	0.10% CMC
	$A_d/A_r^{1.618}$	0.199 ± 0.004 A*	0.199 ± 0.003 A*	0.266 ± 0.003 B*	0.202 ± 0.001 A*	0.267 ± 0.003 B*	
	$A_r/A_d^{1.618}$	0.080 ± 0.002 A	0.114 ± 0.002 B	0.088 ± 0.001 C	0.114 ± 0.002 D	0.133 ± 0.002 E	0.25% CMC
	$A_d/A_r^{1.618}$	0.199 ± 0.004 A*	0.199 ± 0.003 A*	0.199 ± 0.002 A*	0.204 ± 0.001 B*	0.200 ± 0.003 A*	
	$A_r/A_d^{1.618}$	0.066 ± 0.001 A	0.089 ± 0.001 B	0.079 ± 0.001 C	0.100 ± 0.001 D	0.114 ± 0.001 E	0.50% CMC
	$A_d/A_r^{1.618}$	0.159 ± 0.003 A*	0.133 ± 0.002 B*	0.199 ± 0.002 C*	0.200 ± 0.001 C*	0.200 ± 0.003 C*	
t_M (s)	$A_r/A_d^{1.618}$	4.186 ± 0.083 A	4.293 ± 0.058 B*	6.089 ± 0.072 C*	5.403 ± 0.073 D*	5.110 ± 0.067 E	NuT
	$A_d/A_r^{1.618}$	5.183 ± 0.103 A*	4.093 ± 0.055 B	4.093 ± 0.048 B	4.102 ± 0.055 B	5.310 ± 0.069 A*	
	$A_r/A_d^{1.618}$	5.482 ± 0.108 A*	6.389 ± 0.086 B*	7.088 ± 0.084 C*	6.304 ± 0.085 BD*	6.212 ± 0.081 D*	0.10% CMC
	$A_d/A_r^{1.618}$	4.286 ± 0.085 A	4.991 ± 0.067 B	4.093 ± 0.048 C	4.102 ± 0.055 C	4.308 ± 0.056 D	
	$A_r/A_d^{1.618}$	10.166 ± 0.201 A*	7.388 ± 0.099 B*	9.084 ± 0.107 C*	7.204 ± 0.097 D*	6.212 ± 0.081 E*	0.25% CMC
	$A_d/A_r^{1.618}$	6.080 ± 0.120 A	6.189 ± 0.083 A	6.089 ± 0.072 A	5.203 ± 0.070 B	5.210 ± 0.068 B	
	$A_r/A_d^{1.618}$	12.060 ± 0.239 A*	9.085 ± 0.122 B*	10.083 ± 0.119 C*	8.205 ± 0.111 D*	7.414 ± 0.097 E*	0.50% CMC
	$A_d/A_r^{1.618}$	6.179 ± 0.122 A	8.286 ± 0.112 B	6.189 ± 0.073 A	6.204 ± 0.084 A	7.114 ± 0.093 C	
k_La (s^{-1})	$A_r/A_d^{1.618}$	0.065 ± 0.002 A*	0.069 ± 0.001 B*	0.066 ± 0.001 AB*	0.088 ± 0.001 C*	0.118 ± 0.002 D*	NuT
	$A_d/A_r^{1.618}$	0.038 ± 0.001 A	0.024 ± 0.001 B	0.023 ± 0.001 B	0.031 ± 0.001 C	0.030 ± 0.001 C	
	$A_r/A_d^{1.618}$	0.049 ± 0.001 A*	0.052 ± 0.001 B*	0.053 ± 0.001 B*	0.055 ± 0.001 C*	0.058 ± 0.001 D*	0.10% CMC
	$A_d/A_r^{1.618}$	0.028 ± 0.001 A	0.021 ± 0.001 B	0.020 ± 0.001 B	0.028 ± 0.001 A	0.028 ± 0.001 A	
	$A_r/A_d^{1.618}$	0.024 ± 0.001 A*	0.030 ± 0.001 B*	0.038 ± 0.001 C*	0.035 ± 0.001 C*	0.036 ± 0.001 C*	0.25% CMC
	$A_d/A_r^{1.618}$	0.021 ± 0.001 A	0.014 ± 0.001 B	0.019 ± 0.001 A	0.021 ± 0.001 A	0.025 ± 0.001 C	
	$A_r/A_d^{1.618}$	0.011 ± 0.001 A*	0.016 ± 0.001 B*	0.021 ± 0.001 C*	0.020 ± 0.001 C	0.032 ± 0.001 D*	0.50% CMC
	$A_d/A_r^{1.618}$	0.008 ± 0.001 A	0.014 ± 0.001 B	0.011 ± 0.001 C	0.022 ± 0.001 D^0	0.023 ± 0.001 D	

Different letters indicate differences ($p \leq 0.05$) for a same row (i.e., for different airflow and U_G). The * signal indicates difference ($p \leq 0.05$) for a given A_d/A_r pair (i.e., $A_r/A_d^{1.618}$ vs $A_d/A_r^{1.618}$). The value harboring the * signal is the bigger one for a given A_r/A_d or A_d/A_r pair. The number zero indicates no difference ($p > 0.05$) for a given A_r/A_d or A_d/A_r pair. Symbols and abbreviations of variables in the text.

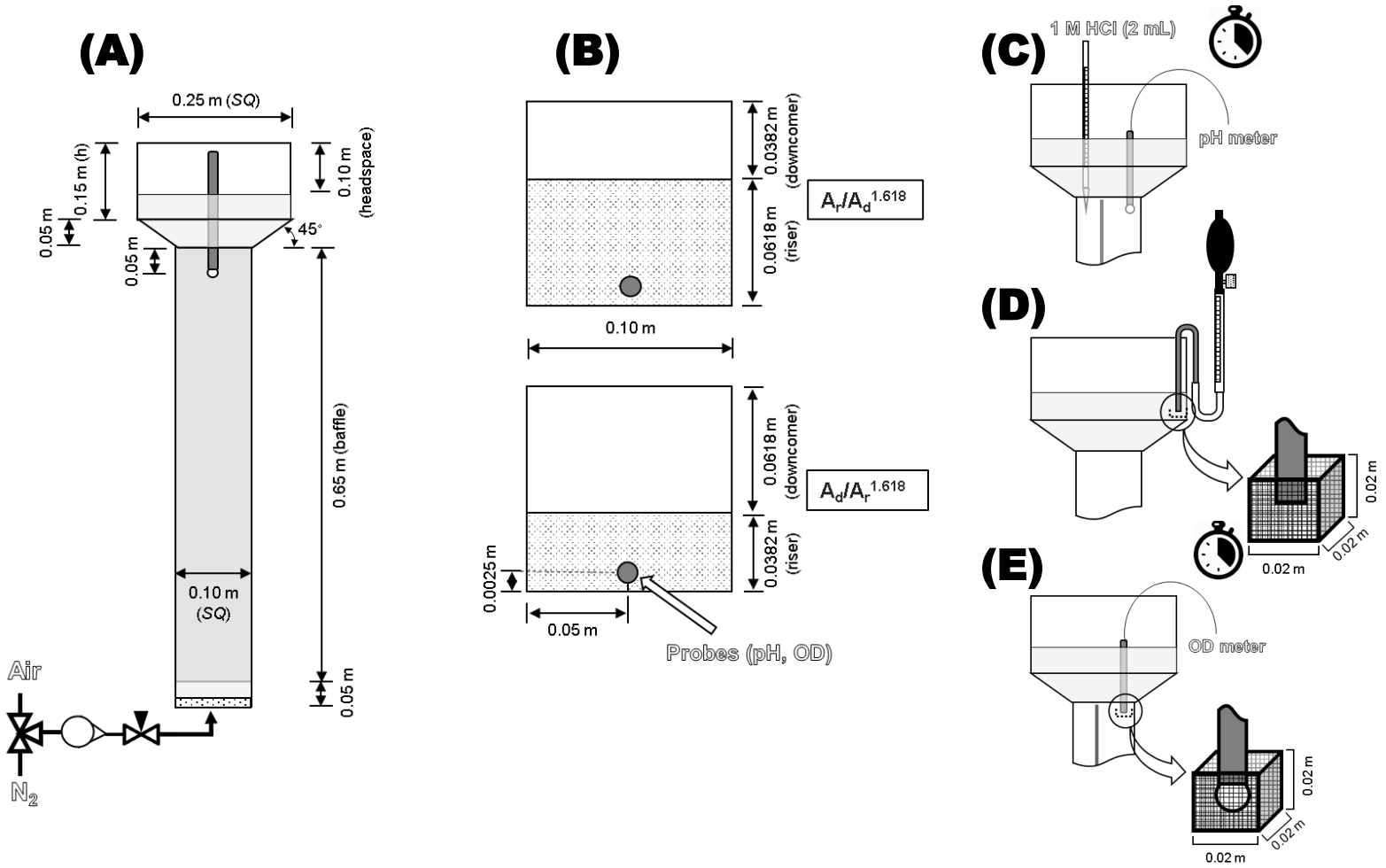

Figure 1. Details of airlift bioreactor and hydrodynamics settings.
(A) Frontal view of SRILAB. **(B)** Cross section of the column with downcomer/riser partition ratios. **(C)** Linear velocity of the liquid (U_L) and mixing time (t_M). **(D)** Gas holdup (ε_g). **(E)** Dissolved oxygen measurements for k_La calculations.

In (D) and (E), a cubic cell was used to avoid entrapment of air/nitrogen bubbles in probe/manometer. It was fabricated with AISI314 stainless steel (ø 0.001 m wire, mesh 0.0053 m, 70% open area). Weldings were carried out with an orthodontic spot welder.

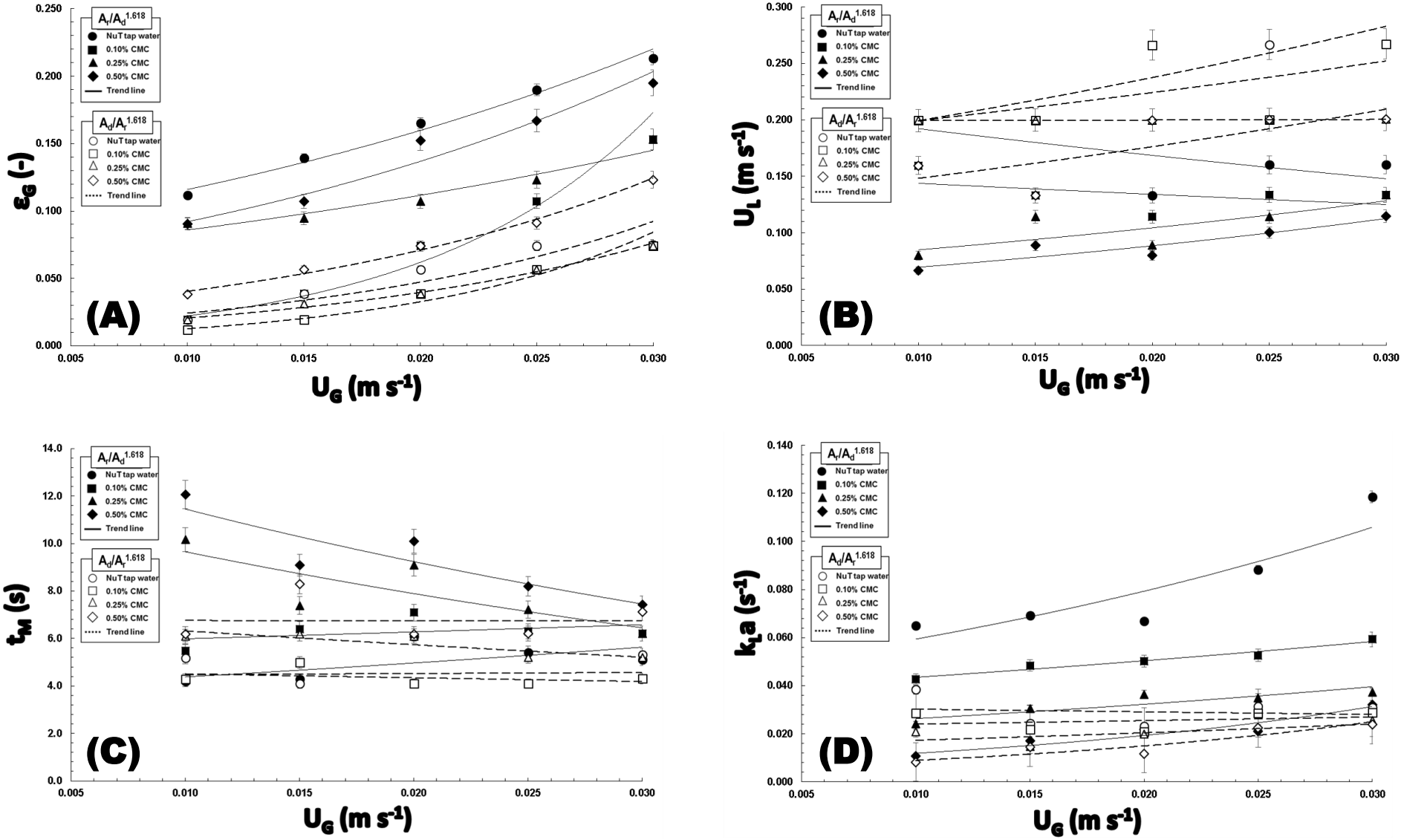

Figure 2. Hydrodynamic and mass transfer parameters for diferente architectures in airlift bioreactor operating with various air flow and Newtonian and non-Newtonian fluids. (A) Curves of ε_G a function of U_G. **(B)** Curves of U_L as a function of U_G. **(C)** Curves of t_M as a function of U_G. **(D)** Curves of k_La as a function of U_G. Error bars denote standard deviations.

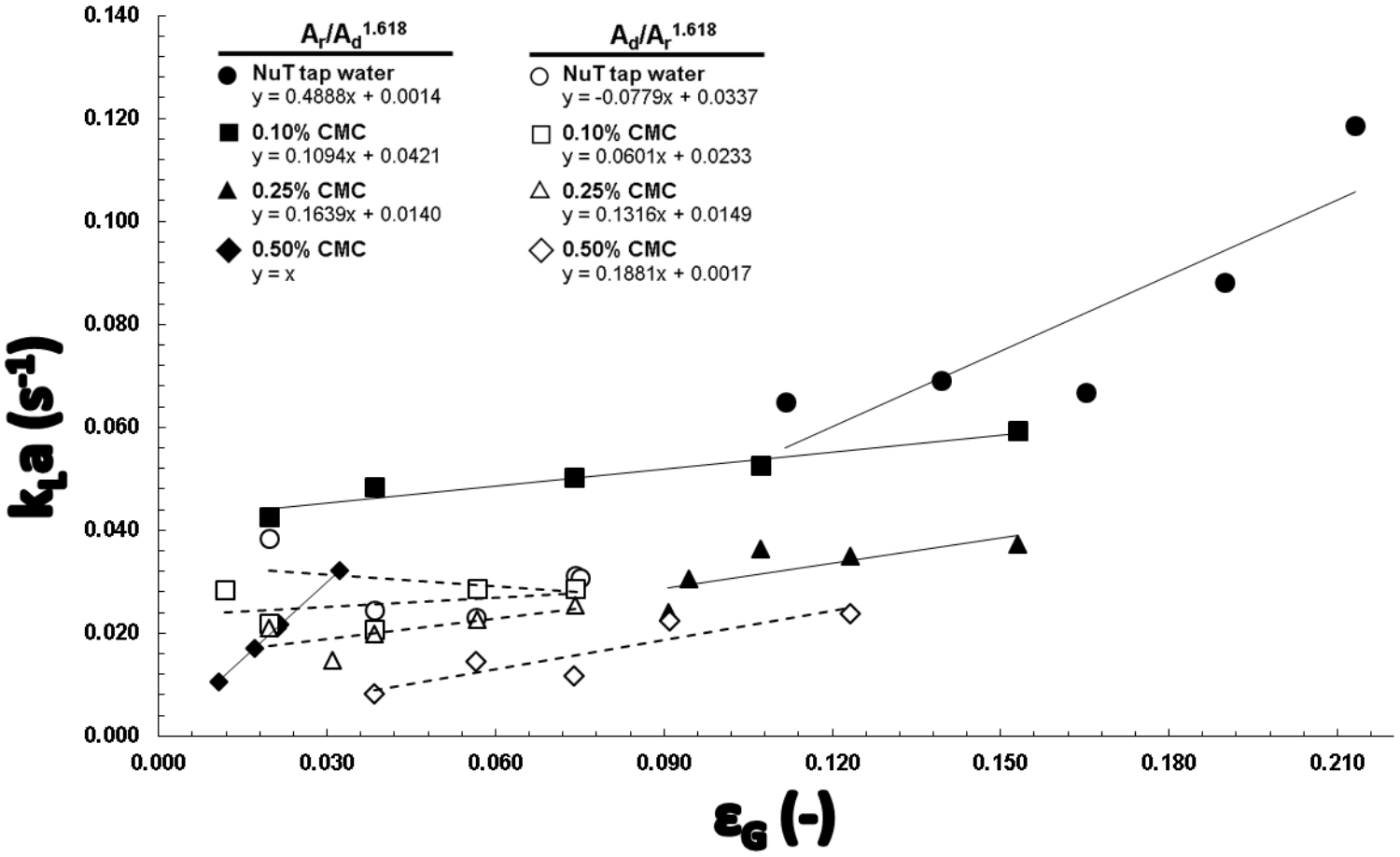

Figure 3. Linear equations derived from plotting k_La vs ε_G.